Article

A New Class of Macrocyclic Lanthanide Complexes for Cell Labeling and Magnetic Resonance Imaging Applications

Quan Zheng, Houquan Dai, Matthew E. Merritt, Craig Malloy, Cai Yuan Pan, and Wen-Hong Li

J. Am. Chem. Soc., **2005**, 127 (46), 16178-16188• DOI: 10.1021/ja054593v • Publication Date (Web): 27 October 2005

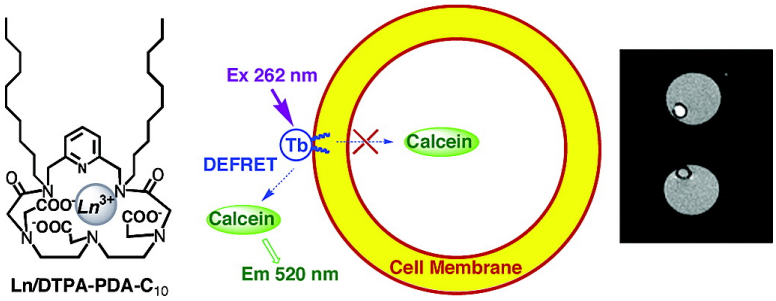

More About This Article

Additional resources and features associated with this article are available within the HTML version:

- Supporting Information
- Links to the 7 articles that cite this article, as of the time of this article download
- Access to high resolution figures
- Links to articles and content related to this article
- Copyright permission to reproduce figures and/or text from this article

View the Full Text HTML

J|A|C|S
ARTICLES
Published on Web 10/27/2005

A New Class of Macrocyclic Lanthanide Complexes for Cell Labeling and Magnetic Resonance Imaging Applications

Quan Zheng,[†,§] Houquan Dai,[†] Matthew E. Merritt,[‡] Craig Malloy,[‡] Cai Yuan Pan,[§] and Wen-Hong Li*[,†]

Contribution from the Department of Polymer Science and Engineering, University of Science and Technology of China, Hefei, Anhui, People's Republic of China, and the Departments of Cell Biology and of Biochemistry and Department of Radiology, University of Texas Southwestern Medical Center at Dallas, Dallas, Texas 75390

Received July 11, 2005; E-mail: wen-hong.li@utsouthwestern.edu

Abstract: Lanthanide complexes have wide applications in biochemical research and biomedical imaging. We have designed and synthesized a new class of macrocyclic lanthanide chelates, Ln/DTPA-PDA-C_n, for cell labeling and magnetic resonance imaging (MRI) applications. Two lipophilic Gd^{3+} complexes, Gd/DTPA−PDA−C_n ($n = 10, 12$), labeled a number of cultured mammalian cells noninvasively at concentrations as low as a few micromolar. Cells took up these agents rapidly and showed robust intensity increases in T1-weighed MR images. Labeled cells showed normal morphology and doubling time as control cells. In addition to cultured cells, these agents also labeled primary cells in tissues such as dissected pancreatic islets. To study the mechanism of cellular uptake, we applied the technique of diffusion enhanced fluorescence resonance energy transfer (DEFRET) to determine the cellular localization of these lipophilic lanthanide complexes. After loading cells with a luminescent complex, Tb/DTPA−PDA−C_{10}, we observed DEFRET between the Tb^{3+} complex and extracellular, but not intracellular, calcein. We concluded that these cyclic lanthanide complexes label cells by inserting two hydrophobic alkyl chains into cell membranes with the hydrophilic metal binding site facing the extracellular medium. As the first imaging application of these macrocyclic lanthanide chelates, we labeled insulin secreting β-cells with Gd/DTPA−PDA−C_{12}. Labeled cells were encapsulated in hollow fibers and were implanted in a nude mouse. MR imaging of implanted β-cells showed that these cells could be followed in vivo for up to two weeks. The combined advantages of this new class of macrocyclic contrast agents ensure future imaging applications to track cell movement and localization in different biological systems.

1. Introduction

Recent progress in the instrumentation and acquisition protocols of magnetic resonance imaging (MRI) has greatly improved the spatial and temporal resolutions of MR images. High field MRI microscopy has been developed to examine living organisms down to the cellular level.[1−5] To fully exploit the advancement of MRI technique for cellular and functional imaging, there are increasing needs for developing new MRI contrast agents and techniques for cell labeling to report the localization, movement, mass, and functions of cells in vivo.[6−8]

Two major classes of contrast agents are available for MRI: macromolecular iron oxide nanoparticles and small molecular weight Gd^{3+} chelates.[9,10] Several techniques have been developed to label cells in vitro with small iron oxide particles and to track labeled cells in vivo.[11−15] These nanosized superparamagnetic iron oxide particulates selectively shorten the transverse relaxation time ($T2$) of nearby water protons and generally

[†] Departments of Cell Biology and of Biochemistry, University of Texas Southwestern Medical Center at Dallas.
[‡] Department of Radiology, University of Texas Southwestern Medical Center at Dallas.
[§] Department of Polymer Science and Engineering, University of Science and Technology of China.

(1) Callaghan, P. T. *Principles of Nuclear Magnetic Resonance Microscopy*; Oxford University Press: New York, 1991.
(2) Blumich, B.; Kuhn, W. *Magnetic Resonance Microscopy*; VCH Publishers: 1992.
(3) Jacobs, R. E.; Papan, C.; Ruffins, S.; Tyszka, J. M.; Fraser, S. E. *Nat. Rev. Mol. Cell Biol.* **2003**, Suppl., SS10−16.
(4) Smith, B. R.; Shattuck, M. D.; Hedlund, L. W.; Johnson, G. A. *Magn. Reson. Med.* **1998**, *39*, 673−677.
(5) Foster-Gareau, P.; Heyn, C.; Alejski, A.; Rutt, B. K. *Magn. Reson. Med.* **2003**, *49*, 968−971.
(6) Louie, A. Y.; Huber, M. M.; Ahrens, E. T.; Rothbacher, U.; Moats, R.; Jacobs, R. E.; Fraser, S. E.; Meade, T. J. *Nat. Biotechnol.* **2000**, *18*, 321−325.
(7) Modo, M.; Cash, D.; Mellodew, K.; Williams, S. C.; Fraser, S. E.; Meade, T. J.; Price, J.; Hodges, H. *Neuroimage* **2002**, *17*, 803−811.
(8) Meade, T. J.; Taylor, A. K.; Bull, S. R. *Curr. Opin. Neurobiol.* **2003**, *13*, 597−602.
(9) Jung, C. W.; Jacobs, P. *Magn. Reson. Imaging* **1995**, *13*, 661−674.
(10) Aime, S.; Botta, M.; Fasano, M.; Terreno, E. *Chem. Soc. Rev.* **1998**, *27*, 19−29.
(11) Yeh, T. C.; Zhang, W.; Ildstad, S. T.; Ho, C. *Magn. Reson. Med.* **1995**, *33*, 200−208.
(12) Frank, J. A.; Miller, B. R.; Arbab, A. S.; Zywicke, H. A.; Jordan, E. K.; Lewis, B. K.; Bryant, L. H., Jr.; Bulte, J. W. *Radiology* **2003**, *228*, 480−487.
(13) Hoehn, M.; Kustermann, E.; Blunk, J.; Wiedermann, D.; Trapp, T.; Wecker, S.; Focking, M.; Arnold, H.; Hescheler, J.; Fleischmann, B. K.; Schwindt, W.; Buhrle, C. *Proc. Natl. Acad. Sci. U.S.A.* **2002**, *99*, 16267−16272.
(14) Lewin, M.; Carlesso, N.; Tung, C. H.; Tang, X. W.; Cory, D.; Scadden, D. T.; Weissleder, R. *Nat. Biotechnol.* **2000**, *18*, 410−414.
(15) Bulte, J. W.; Douglas, T.; Witwer, B.; Zhang, S. C.; Strable, E.; Lewis, B. K.; Zywicke, H.; Miller, B.; van Gelderen, P.; Moskowitz, B. M.; Duncan, I. D.; Frank, J. A. *Nat. Biotechnol.* **2001**, 19, 1141−1147.

10.1021/ja054593v CCC: $30.25

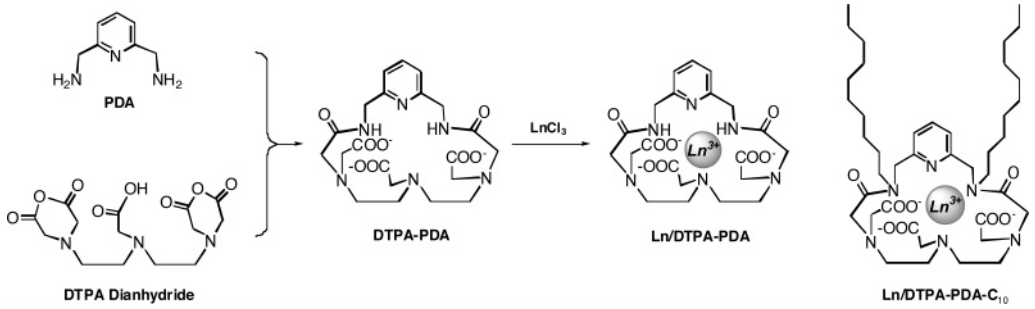

Figure 1. A new class of macrocyclic lanthanide complexes, Ln/DTPA−PDA, and a hydrophobic homologue Ln/DTPPA−PDA−C_{10}.

produce negative enhancement by decreasing signal intensity. Since the *T*2 relaxation time of tissues is generally short, the contrast enhancement by iron oxide particles can be limited. Commonly used Gd^{3+} complexes such as Gd-DTPA and Gd-DOTA efficiently shorten the longitudinal relaxation time (*T*1) of water protons and increase the signal intensity of MR images. Since these Gd^{3+} chelates are charged and hydrophilic molecules, they are impermeable to cell membranes and are taken up by cells very slowly. Recent attempts of labeling cells with Gd^{3+} chelates mainly involve using cell translocation peptides such as HIV-tat peptides[16] or polyarginine peptides.[17] These translocation peptides have been shown to be capable of shuttling a variety of cargos across cell membranes through mechanisms that are not well understood.

Instead of targeting intracellular compartments, we envisioned a different approach of labeling cells by tagging cell membranes with *T*1 agents. Lipophilic fluorescent dyes such as DiI or DiO have been used extensively in cell labeling and fluorescence imaging.[18] The technique was originally developed for labeling cultured neurons to study cell−cell interactions during axonal outgrowth and synaptogenesis.[19] The application of this technique has later been extended to labeling cells in situ in living organisms including developing embryos and adult animals. Labeled cells remain visible in vivo by fluorescence microscopy for an extended period of time.[20−22] Lipophilic Gd^{3+} complexes that can be stably incorporated into cell membranes may serve as magnetic dyes for cell labeling and cell tracking. Ideally, these Gd^{3+} chelates should label intact cell membranes noninvasively at low concentrations and with fast kinetics, and should remain on labeled cells over a period of time to allow repetitive imaging.

We have developed a new class of macrocyclic lanthanide complexes, Ln/DTPA−PDA−C_n, for cellular labeling and imaging applications. The lipophilicity of these agents can be systematically modified by using alkyl chains of varied lengths. When these hydrophobic Gd^{3+} complexes are added to cell culture at concentrations as low as a few micromolar, cells take up these agents rapidly and show robust intensity increases in *T*1-weighed MR images. In addition to cultured cells, these agents also label primary cells in tissues such as dissected pancreatic islets. To study the mechanism of cellular uptake, we applied the technique of diffusion enhanced fluorescence resonance energy transfer (DEFRET) to determine the cellular localization of these lipophilic lanthanide complexes. We concluded from these studies that this new class of cyclic lanthanide complexes label cells by inserting two hydrophobic alkyl chains into cell membranes with the hydrophilic metal binding site facing the extracellular medium. As the first imaging application of these macrocyclic lanthanide chelates, we labeled insulin secreting β-cells with a lipophilic Gd^{3+} complex. Labeled cells were encapsulated in hollow fibers and were implanted in a nude mouse. MR imaging of implanted β-cells showed that these cells could be followed in vivo for up to two weeks.

2. Results

2.1. Design and Synthesis. We designed a new class of cyclic lanthanide complexes based on two known metal ligands: diethylenetriamine pentaacetate (DTPA) and 2,6-pyridinedimethaneamine (PDA). Macrocyclization of DTPA dianhydride and PDA provides a multivalent chelator, DTPA−PDA (Figure 1). Molecular modeling indicated that lanthanide ions (Ln^{3+}) such as Gd^{3+} or Tb^{3+} fit nicely into the center cavity of the macrocycle. The resulting complex, Ln/DTPA−PDA, is overall neutral. The pyridine ring shields the top half of the complex, partially reducing the hydrophilicity around Ln^{3+} ion. To further enhance the hydrophobicity of the metal chelate, and to promote the association of the complex to cell plasma membranes, we replace each of the hydrogen atoms of primary pyridinedimethaneamines with an alkyl group. We named these hydrophobic homologues Ln/DTPA−PDA−C_n, with "C_n" denoting the number of carbon atoms of the linear alkyl chain on the nitrogen atom of secondary amide.

DTPA−PDA−C_n were synthesized from 2,6-bis(bromomethyl) pyridine in five steps (Figure 2). To determine how the alkyl chain length and the overall hydrophobicity of the compound affect cell labeling, we prepared three chelates with increasing alkyl chain length: butyl, decyl, and dodecyl alkyl groups (R = C_4H_9, $C_{10}H_{21}$, or $C_{12}H_{25}$, Figure 2). Nucleophilic substitution of 2,6-bis(bromomethyl)pyridine with primary amines yielded *N*,*N*′-dialkyl PDA derivatives **1a**−**1c**. Excess amount of primary amines were used in these reactions to minimize the formation of tertiary amines. Initially we attempted to separate compounds **1a**−**1c** from excess primary amines using the silica gel chromotography. Later, we found that it was easier to purify these intermediates indirectly as their trifluoroacetamides **2a**−**2c**. Basic hydrolysis of purified trifluoroacetamides **2a**−**2c** provided pyridine diamines **1a**−**1c** in quantitative yields. These diamines were reacted in situ with DTPA dianhydride to

(16) Bhorade, R.; Weissleder, R.; Nakakoshi, T.; Moore, A.; Tung, C. H. *Bioconjug. Chem.* **2000**, *11*, 301−305.
(17) Allen, M. J.; MacRenaris, K. W.; Venkatasubramanian, P. N.; Meade, T. J. *Chem. Biol.* **2004**, *11*, 301−307.
(18) Honig, M. G.; Hume, R. I. *Trends Neurosci.* **1989**, *12*, 336−338.
(19) Honig, M. G.; Hume, R. I. *J. Cell Biol.* **1986**, *103*, 171−187.
(20) Vidal-Sanz, M.; Villegas-Perez, M. P.; Bray, G. M.; Aguayo, A. J. *Exp. Neurol.* **1988**, *102*, 92−101.
(21) Kulesa, P. M.; Fraser, S. E. *Development* **2000**, *127*, 1161−1172.
(22) Timmers, M.; Vermijlen, D.; Vekemans, K.; De Zanger, R.; Wisse, E.; Braet, F. *J. Microsc.* **2002**, *208*, 65−74.

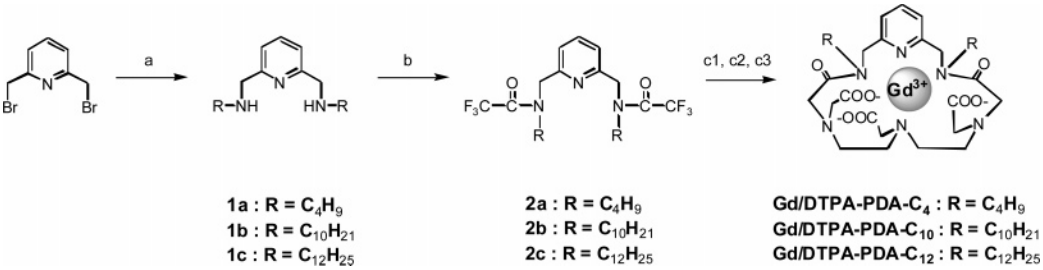

Figure 2. Syntheses of three macrocyclic MRI contrast agents Gd/DTPA−PDA−C_n (n = 4,10,12). a. *n*-Butylamine, toluene, **1a**; or *n*-decylamine, **1b**; or *n*-dodecylamine, **1c**; b. $(CF_3CO)_2O$, CH_3CN, K_2CO_3, 50∼70% for steps a and b; c. (1) NaOH(aq.), THF; (2) DTPA dianhydride, DMF, 25∼39% for 2 steps; (3) $GdCl_3$, 0.1 N NaOH, pH 6.5, MeOH/H_2O.

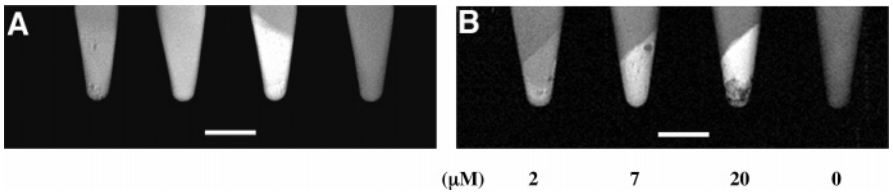

Figure 3. Cell labeling and MRI contrast enhancement by Gd/DTPA−PDA−C_n. (**A**) Four tubes containing (from left to right) control unlabeled Hela cells, Hela cells labeled with Gd/DTPA−PDA−C_4 (10 μM, 40 min), Hela cells labeled with Gd/DTPA−PDA−C_{10} (10 μM, 40 min), and HBS, were imaged together in a Varian Unity INOVA imaging system equipped with an Oxford 4.7 T magnet. The image, shown as raw data, was acquired with a standard spin−echo sequence with a repetition time (TR) of 300 ms and an echo time (TE) of 30 ms. (**B**) Gd/DTPA−PDA−C_{12} enhances the intensity of MR images of labeled cells dose dependently. Hela cells were labeled with Gd/DTPA−PDA−C_{12} for 40 min at indicated concentrations (μM). After washing, cells were spun down to the bottom of vials and imaged similarly as in A. TR/TE = 300/25 ms. The scale bar is 6 mm.

form the macrocyclic ligands. Formation of Gd^{3+} complexes was carried out under weakly acidic conditions.

2.2. Cell Labeling and in Vitro MR Imaging of Labeled Cells. To determine the efficiency of cellular uptake and MRI contrast enhancement of this series of macrocyclic lanthanide complexes, we labeled cultured mammalian cells with Gd^{3+} complexes and imaged these cells by MRI. Stock solutions of Gd/DTPA−PDA−C_n (n = 4, 10, 12) were added to Hela cells bathed in the Hanks Balanced Saline (HBS, supplemented with 20 mM Hepes, 5.5 mM glucose, pH 7.3). Cells were then incubated with the Gd^{3+} complexes at room temperature for 30−40 min. After washing cells with HBS, we detached cells from Petri dishes using trypsin and spun cells down in small vials (0.6 mL). Labeled cell pellets were then imaged together with control cells. *T*1-weighed imaging showed that Hela cells labeled with Gd/DTPA−PDA−C_{10} were remarkably brighter than cells labeled with Gd/DTPA−PDA−C_4 or control cells (Figure 3A). The image intensities of cells labeled with Gd/DTPA−PDA−C_4 and unlabeled cells were comparable, and they were fairly close to that of HBS alone. These results suggested that Gd/DTPA−PDA−C_{10} was taken up by cells efficiently, and the compound was fairly effective in enhancing the contrast of MR images. Another Gd^{3+} complex, Gd/DTPA−PDA−C_{12}, enhanced the intensity of MR images of labeled Hela cell similarly as Gd/DTPA−PDA−C_{10}. Since Gd/DTPA−PDA−C_4 produced little contrast enhancement, this suggests that the efficiency of cellular uptake of this chelate is much lower than the other two metal complexes, most likely due to its low hydrophobicity.

To investigate how the extracellular concentration of lipophilic Gd^{3+} complexes affects cell labeling, we labeled cells with Gd/DTPA−PDA−C_{12} at different doses and compared MR images of these cells. Cells labeled with 20 μM of Gd/DTPA−PDA−C_{12} showed a very strong signal in *T*1-weighed imaging (Figure 3B). Decreasing the loading concentration of Gd/DTPA−PDA−C_{12} diminishes the signal intensity of MR images. Remarkably, even at the loading concentration of 2 μM, labeled cells still showed visible contrast enhancement over control cells (Figure 3B). Moreover, once taken up by cells, Gd/DTPA−PDA−C_{12} did not appear to cause gross toxicity. These labeled cells can be further cultured, showing normal morphology and doubling time as control cells over at least a week.

We also tested Gd/DTPA−PDA−C_{10} and Gd/DTPA−PDA−C_{12} in a number of other cell lines including COS cells, NIH-3T3 cells, rat gliosarcoma cells, and insulin secreting INS-1 β-cells (vide infra). All these cells took up Gd/DTPA−PDA−C_{10} and Gd/DTPA−PDA−C_{12} efficiently and they showed significant contrast enhancement by MR imaging. In addition to adhering cells, Gd/DTPA−PDA−C_{10} and Gd/DTPA−PDA−C_{12} also labeled nonadhering cells such as T-lymphocyte Jurkat cells (Figure S1, Supporting Information). Thus, the labeling and contrast enhancement properties of these lipophilic lanthanide complexes appeared to be fairly general for cultured mammalian cells.

2.3. Mechanistic Studies of the Cellular Uptake and Contrast Enhancement. The efficient cellular labeling and contrast enhancement by this new class of cyclic lanthanide complexes prompted us to study the mechanism of cellular uptake and their mode of actions. To quantify the cellular enrichment and to study the cellular localization of these lipophilic lanthanide complexes, we prepared corresponding Tb^{3+} complexes, Tb/DTPA−PDA−C_n (n = 4, 10, and 12). Lanthanide ions, Tb^{3+} and Eu^{3+} ions in particular, possess extraordinary luminescent properties including very long luminescence lifetimes on the order of millisecond, large Stokes' shift, and distinguished and sharp emission peaks.[23] Because of their long luminescence lifetimes, Eu^{3+} and Tb^{3+} complexes offer high sensitivity of detection in the time-resolved mode in which short-lived background fluorescence is rejected by the

(23) Richardson, F. S. *Chem. Rev.* **1982**, *82*, 541−552.

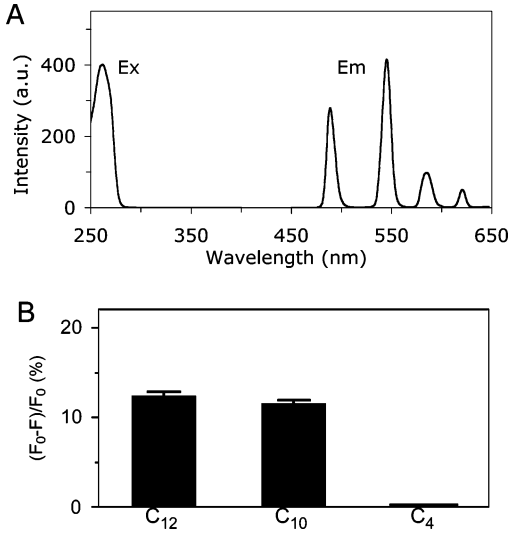

Figure 4. Measure cellular uptake of cyclic Tb^{3+} complexes using time-resolved luminescence. (A) Time-resolved excitation ($E_m = 545$ nm) and emission spectra ($E_x = 262$ nm) of Tb/DTPA−PDA−C_{10} in HBS (pH 7.30). (B) Cellular uptake of Tb/DTPA−PDA−C_n ($n = 4$, 10, or 12) measured from the change of Tb^{3+} luminescence. Jurkat cells were incubated with Tb/DTPA−PDA−C_n (10 μM) for 40 min in HBS. F_0 is the initial luminescence intensity at 545 nm before cells were added, F is the luminescence intensity at 545 nm of the supernatant after loading. $(F_0 - F)/F_0$ measures the percentage of Tb/DTPA-PDA-C_n taken up by cells. All measurements were made on a LS-55 Luminescence Spectrometer (Perkin-Elmer) with a delay time (t_d) of 0.1 ms and a gate time (t_g) of 1 ms. Error bars represent standard deviations of three measurements.

temporal gating.[24] In addition, luminescent Tb^{3+} and Eu^{3+} chelates serve as efficient energy donors in the diffusion enhanced fluorescence resonance energy transfer (FRET).[25] This unique property can be exploited to investigate the localization of luminescent lanthanide complexes in biological systems (vide infra).

The time-resolved excitation and emission spectra of Tb/DTPA−PDA−C_{10} are shown in Figure 4A. The peak excitation wavelength is at 262 nm. The absorption spectra of the complex and of the free ligand DTPA−PDA−C_{10} (Figure S2, Supporting Information) are similar to the excitation spectrum of Tb/DTPA−PDA−C_{10}, suggesting that pyridine acts as an antenna and transfers the absorbed photonic energy to the nearby Tb^{3+} ion. Ln^{3+} ions by themselves are rather inefficient in absorbing light. The sensitized excitation from pyridine greatly increases the effective extinction coefficient of Tb^{3+} and therefore boosts the luminescence intensity of the complex. The primary emission peak of Tb/DTPA−PDA−C_{10} centers around 545 nm. This emission peak results from the $^5D_4 \rightarrow {}^7F_5$ transition of 4*f* electrons of Tb^{3+} ion.[23] The excitation and emission spectra of Tb/DTPA−PDA−C_4 and Tb/DTPA−PDA−C_{12} are identical with those of Tb/DTPA−PDA−C_{10}, and the luminescence intensity of these complexes changes little in HBS buffer (containing 1.26 mM Ca^{2+}) during the measurement, suggesting that these complexes are stable in physiological solutions.

To estimate the amount of Tb^{3+} complexes taken up by cells, we loaded human T-lymphocyte Jurkat cells with Tb/DTPA−PDA−C_n ($n = 4$, 10, and 12). After measuring the initial luminescence intensity of Tb^{3+} emission at 545 nm in the loading solution, we added cells to start cellular uptake of the complexes. About 40 min later, we removed cells by centrifugation and remeasured the luminescence intensity of the supernatant at 545 nm. The decrease in the luminescence intensity of the loading solution corresponded to the amount of Tb^{3+} complexes taken up by cells. The results showed that more than 10% of Tb/DTPA−PDA−C_{10} and Tb/DTPA−PDA−C_{12} were taken up by cells after 40 min of incubation, whereas Tb/DTPA−PDA−C_4 largely remained in the loading solution (Figure 4B). This result was consistent with the MRI data showing that Gd/DTPA−PDA−C_4 failed to enhance the contrast of MR images.

To study the cellular localization of these complexes taken up by cells, we resorted to the technique of diffusion enhanced fluorescence resonance energy transfer (DEFRET). FRET results from electronic dipole−dipole interactions of a donor and a suitable acceptor chromophore. Conventional FRET occurs when a pair of suitable organic fluorophores are located within a distance of 80 Å or less, and it mainly detects dipole interactions within a molecule or in a tightly packed molecular complex. Chromophores with long fluorescence lifetimes can diffuse over a distance within the lifetime of their excited states. A donor and an acceptor that are too far apart for FRET at the moment of excitation can be brought into close proximity by diffusion. During the excited-state lifetime of a donor, if the donor and/or the acceptor can diffuse over a distance comparable to or greater than the mean distance between them, the efficiency of *intermolecular* energy transfer can be greatly enhanced by diffusion.[25] Tb^{3+} and Eu^{3+} complexes have luminescence lifetimes on the order of millisecond, about a million times longer than common organic fluorophores. Since diffusion constants of small molecules in aqueous solutions are typically 1×10^{-5} cm^2/sec, the efficiency of DEFRET approaches a maximal value in the rapid diffusion limit, i.e, $D\tau_0 \gg s^2$, where D is the sum of the diffusion coefficients of the donor and acceptor, τ_0 is the lifetime of the donor in the absence of energy transfer, and s is mean distance between donors and acceptors. Stryer and co-workers predicted and demonstrated that DEFRET between freely diffusing terbium dipicolinate and rhodamine B occurred efficiently in aqueous solutions even at micromolar concentrations.[26]

An important feature of DEFRET is that the efficiency of energy transfer is extremely sensitive to the distance of closest approach of diffusing donors and acceptors. In aqueous solutions, the rate of energy transfer is inversely proportional to the cubic power of the distance between diffusing luminescent lanthanide complexes and acceptors. This property has been exploited to study the localization of chromophores in proteins or membranes.[25,27,28]

To apply the technique of DEFRET to investigate the cellular localization of Tb/DTPA−PDA−C_{10}, we chose calcein as the energy acceptor for two reasons. First, the excitation spectrum of calcein overlaps with the Tb^{3+} emission peak centered at 490 nm (Figure 5A). Such a spectral overlap is required for efficient dipole energy transfer. Second, calcein is a highly charged and hydrophilic molecule at physiological pH and is

(24) Hemmila, I.; Mukkala, V. M. *Crit. Rev. Clin. Lab. Sci.* **2001**, *38*, 441−519.
(25) Stryer, L.; Thomas, D. D.; Meares, C. F. *Annu. Rev. Biophys. Bioeng.* **1982**, *11*, 203−222.
(26) Thomas, D. D.; Carlsen, W. F.; Stryer, L. *Proc. Natl. Acad. Sci.* **1978**, *75*, 5746−5750.
(27) Thomas, D. D.; Stryer, L. *J. Mol. Biol.* **1982**, *154*, 145−157.
(28) Wensel, T. G.; Chang, C. H.; Meares, C. F. *Biochemistry* **1985**, *24*, 3060−3069.

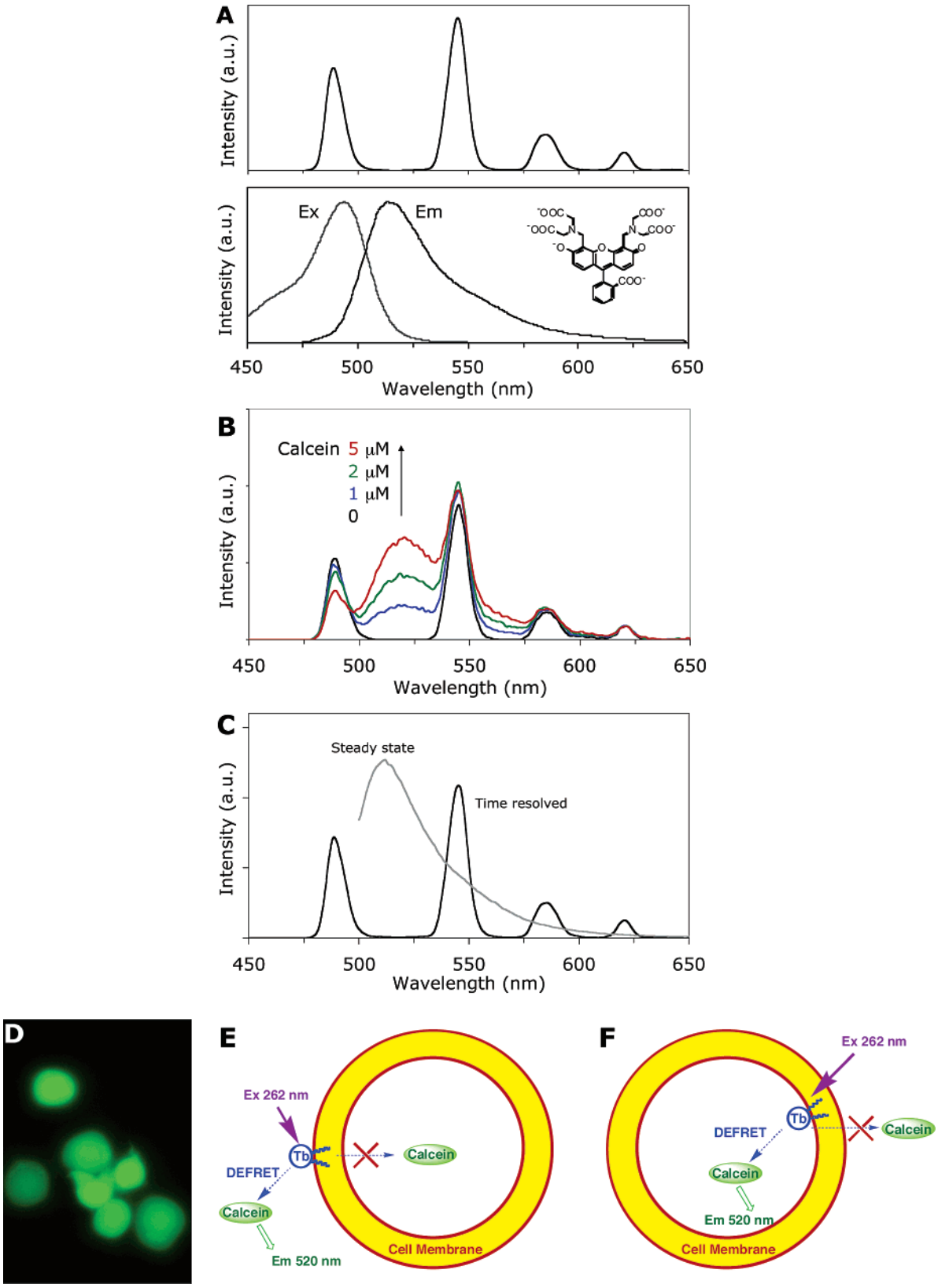

Figure 5. Probe cellular localization of Tb/DTPA−PDA−C_{10} by DEFRET. (A) The spectral overlap of Tb/DTPA−PDA−C_{10} emission (upper trace) and calcein excitation (lower trace, calcein structure also shown). (B) DEFRET between extracellular calcein and Tb/DTPA−PDA−C_{10} taken up by cells. Increasing amounts of calcein were added to a suspension of Jurkat cells loaded with Tb/DTPA−PDA−C_{10}. Time-resolved emission spectra (E_x = 262 nm, t_d = 0.1 ms, t_g = 1 ms) were acquired after each addition of calcein. (C) No DEFRET was observed between intracellular calcein and Tb/DTPA−PDA−C_{10} taken up by cells. Jurkat cells were loaded with calcein/AM (1 μM) and Tb/DTPA−PDA−C10 (10 μM) for 40 min. Calcein emission could only be detected in the steady state (E_x = 490 nm). (D) A fluorescence image (E_x 490 ± 10 nm, E_m 530 ± 20 nm) of Jurkat cells loaded with calcein/AM. (E, F) Illustrations of DEFRET between calcein and Tb/DTPA−PDA−C_{10} with respect to their cellular localizations. DEFRET to extracellular calcein occurs when Tb^{3+} complexes face the extracellular medium (E); and DEFRET to intracellular calcein can only be observed when Tb^{3+} complexes translocate to the cytosol (F).

impermeable to cell membranes. However, it can be delivered inside cells by using Calcein/AM, a neutral ester of calcein that is hydrolyzed by cellular esterases to generate calcein intracellularly. This would allow us to control the localization of calcein by using either calcein or calcein/AM, and to investigate the cellular localization of Tb/DTPA−PDA−C_{10} through DEFRET.

After loading Jurkat cells with Tb/DTPA−PDA−C_{10}, we washed cells several times and resuspended them in HBS. Time-resolved spectra of the cell suspension showed characteristic Tb^{3+} emission (Figure 5B, calcein = 0 μM). After calcein was added, a broad peak corresponding to the calcein emission appeared between 500 and 530 nm. Since all the spectra were acquired in the time-resolved mode with a delay time of 0.1 ms, the observed calcein emission between 500 and 530 nm must be through energy transfer from Tb/DTPA−PDA−C_{10}. Adding more calcein to the cell suspension increased the emission intensity between 500 and 530 nm, and it decreased the intensity of Tb^{3+} emission at 490 nm correspondingly. This is consistent with the theory of DEFRET which states that the rate of intermolecular energy transfer in solutions increases linearly with the concentration of acceptors.[25]

In contrast, when calcein was delivered inside cells using calcein-AM, calcein emission was only detected by the steady-state fluorescence spectroscopy, but not by the gated detection (Figure 5C). The intracellular localization of calcein was also confirmed by the fluorescence microscopy (Figure 5D). Since calcein emission was undetectable in the time-resolved mode, it suggested that no energy transfer has occurred between intracellular calcein and Tb/DTPA−PDA−C_{10}. The efficiency of diffusion enhanced energy transfer falls off with the cubic power of the distance of closest approach of diffusing donors and acceptors.[25] The lack of energy transfer must indicate that Tb/DTPA−PDA−C_{10} is separated from intracellular calcein by a barrier which prevents any significant dipole interactions.

On the basis of the results from DEFRET, we conclude that cells take up Tb/DTPA−PDA−C_{10} mainly through hydrophobic interactions between cell membranes and two alkyl chains of the lanthanide complex. Once taken up by cells, Tb/DTPA−PDA−C_{10} adopts a configuration in which decyl alkanes insert into the out leaflet of membrane lipid layer, and the hydrophilic Tb^{3+} chelate faces the extracellular medium (Figure 5E). In this topology, DEFRET between Tb/DTPA−PDA−C_{10} and extracellular calcein occurs readily because the distance of closest approach between them is only limited by the van der Waals radius of each molecule. When calcein is delivered inside cells, DEFRET from Tb/DTPA−PDA−C_{10} would be minimum because the distance of the closest approach between intracellular calcein and Tb/DTPA−PDA−C_{10} is limited by the lipid bilayer of cell membranes, about 75 Å thick. Our data also suggests that a different localization, in which Tb/DTPA−PDA−C_{10} flip-flops to the inner leaflet of lipid bilayer with the Tb^{3+} chelator facing cytosol (Figure 5F), is unlikely.

Once taken up by cells, Tb/DTPA−PDA−C_{10} should remain tightly associated with the cell membranes. Since the hydrophilic metal binding cavity of the macrocyclic complex is shielded by hydrophobic moieties—an aromatic ring and two alkyl chains, we speculate that most of the methylene groups of two alkyl chains (and perhaps part of the pyridine ring) are immersed in the lipid layer. In addition, the complex is overall neutral, so there should be little charge repulsion between the complex and the polar headgroups of phospholipids. Other lanthanide complexes of DTPA−PDA−C_n with long alkyl chains should be taken up by cells similarly as Tb/DTPA−PDA−C_{10}. The striking image contrast enhancement from Gd/DTPA−PDA−C_n ($n \geq 10$) can be attributed to at least two factors. First, these lipophilic Ln^{3+} complexes get enriched in cells efficiently. Luminescence measurements showed that about 10% of Tb/DTPA−PDA−C_{10} or Tb/DTPA−PDA−C_{12} was taken up by cells after 40 min incubation (Figure 4B). The amount of Tb/DTPA−PDA−C_{10} or Tb/DTPA−PDA−C_{12} enriched in cells was estimated to be more than a hundred times higher than the bulk concentration in the loading solution and could reach millimolar range. Second, once taken up by cells, the movement of these cyclic lanthanide complexes is limited to the lateral diffusion in the lipid layer. Two long alkyl chains are inserted in the cell membrane. This conformation effectively restricts the movement of cyclic lanthanide complexes and slows down their molecular tumbling rates. It is known that the longitudinal relaxivity of small Gd^{3+} chelates can increase significantly when there is an increase in their rotational correlation time (τ_r).[29] This property has been exploited to improve the relaxivity of contrast agents by conjugating small Gd^{3+} chelates to macromolecular carriers.[29−31] MS-325, a blood pool MRI contrast agent, binds to human serum albumin in plasma through a hydrophobic bisphenylcyclohexyl group.[32] The association with serum albumin reduces the rotational rate of MS-325 by a factor of 100, and increases its relaxivity up to 10 times.[32] Since there should be a sizable increase in τ_r of lipophilic Gd/DTPA−PDA−C_n ($n \geq 10$) after the agent adheres to cell membranes, and because τ_r affects the longitudinal relaxivity of Gd^{3+} contrast agents most effectively at the field strength between 0.2 T and 2 T,[29] we expect that Gd/DTPA−PDA−C_n ($n \geq 10$) will be even more effective in enhancing the contrast of MR images at magnetic fields lower than what we used in this study (4.7 T). Future investigations of the field dependence of relaxation rates (nuclear magnetic relaxation dispersion profile, or NMRD[33]) of this new class of contrast agents should offer further mechanistic insights on their mode of actions.

2.4. MR Imaging of Beta-Cells in Vitro and in Implanted Nude Mice. As the first in vivo application of this new class of lipophilic lanthanide complexes, we used them to label insulin secreting β-cells and imaged labeled cells in host animals after implantation. The β-cells of the islets of Langerhans play crucial roles in regulating metabolism through the action of secreting insulin. The malfunction of insulin secretion and/or insulin action is manifested as diabetes mellitus.[34,35] In type 1 diabetes, pancreatic β-cells are destructed by autoimmune reactions; and in type 2 diabetes, β-cells are gradually injured. To understand the mechanisms of β-cell loss and to follow intervention therapies, there are growing interests in developing noninvasive

(29) Caravan, P.; Ellison, J. J.; McMurry, T. J.; Lauffer, R. B. *Chem. Rev.* **1999**, *99*, 2293−2352.
(30) Spanoghe, M.; Lanens, D.; Dommisse, R.; Van der Linden, A.; Alderweireldt, F. *Magn. Reson. Imaging* **1992**, *10*, 913−917.
(31) Wiener, E. C.; Brechbiel, M. W.; Brothers, H.; Magin, R. L.; Gansow, O. A.; Tomalia, D. A.; Lauterbur, P. C. *Magn. Reson. Med.* **1994**, *31*, 1−8.
(32) Caravan, P.; Cloutier, N. J.; Greenfield, M. T.; McDermid, S. A.; Dunham, S. U.; Bulte, J. W.; Amedio, J. C., Jr.; Looby, R. J.; Supkowski, R. M.; Horrocks, W. D., Jr.; McMurry, T. J.; Lauffer, R. B. *J. Am. Chem. Soc.* **2002**, *124*, 3152−3162.
(33) Muller, R. N.; Vanderelst, L.; Rinck, P. A.; Vallet, P.; Maton, F.; Fischer, H.; Roch, A.; Vanhaverbeke, Y. *Invest. Radiol.* **1988**, *23*, S229−S231.
(34) Larger, E.; Dubois-Laforgue, D. *Ann. Med. Interne* **1999**, *150*, 254−263.
(35) Hales, C. N. *Brit. Med. Bull.* **1997**, *53*, 109−122.

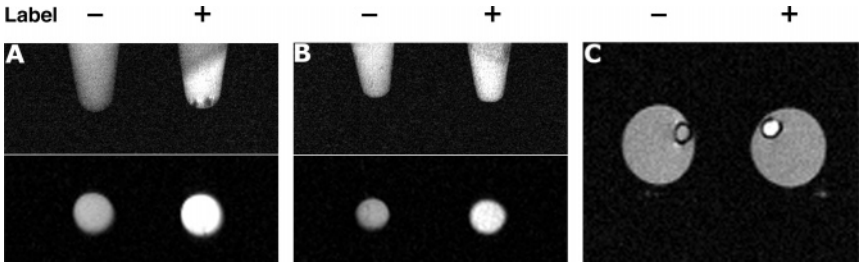

Figure 6. T_1-weighed MR images of INS-1 cells and human islets labeled with Gd/DTPA−PDA−C_{12}. (A and B) Longitudinal and transaxial images of INS-1 clonal (832/13) cells (A) or human islets (B) in small vials. (C) A transaxial image of INS-1 clonal (832/13) cells in implant hollow fibers (I.D. = 1.0 mm, O.D. = 1.2 mm) placed inside glass tubes (I.D. = 4.5 mm) filled with water. TR/TE = 300/30 ms for (A) and (B), and TR/TE = 150/25 ms for (C). Cells or human islets were labeled with Gd/DTPA−PDA−C_{12} (20 μM) for about an hour.

imaging techniques to follow the mass and function of β-cells in vivo.[36−40] Traditional methods of dissection and histology rarely give dynamic information of β-cell physiology over their natural life spans. In addition to imaging endogenous islet β-cells, there are also needs for imaging implanted β-cells or islets. Beta-cell transplantation using either islets or engineered β-cells offers promises in restoring regulated insulin release in hosts whose endogenous islet β-cells have been damaged.[41,42] In the course of developing these transplantation procedures, it would be tremendously beneficial for physicians to follow the localization and fate of implanted cells continuously over a period of time. MRI is ideally suited for tracking β-cells because of its high spatial resolution.

Gd/DTPA-PDA-C_{12} labels INS-1 cells as efficiently as it labels other types of cells. Labeled β-cells showed significant contrast enhancement over control cells by *T*1-weighed MRI (Figure 6A). To address the question whether this class of contrast agents is able to label primary cells in tissues, we incubated dissected human islets with Gd/DTPA−PDA−C_{12} for about an hour. After washing, we spun down islets to the bottom of a small vial and imaged them together with control islets. Labeled islets were brighter than control islets by *T*1-weighed MR imaging (Figure 6B), yet the contrast enhancement appeared to be slightly lower than that observed in cultured β-cells (Figure 6A). The difference probably results from the fact that cells are packed much more tightly in tissues than in culture. It would take longer time for Gd/DTPA−PDA−C_{12} to diffuse into islets and to label cells beneath the surface. Increasing the concentration of contrast agents and/or loading time should produce higher contrast enhancement in tissues.

To track β-cells in living animals, we labeled INS-1 cells and encapsulated them in hollow fibers. These fibers are made of modified poly(vinylidene difluoride) membranes with a molecular weight cutoff of 500 000. Small metabolites, nutrients, oxygen, and most proteins can diffuse in and out of membranes, but cells remain to be trapped inside. After labeling and washing, cells were suspended in a small volume of HBS and injected inside the fiber membrane using a syringe. Labeled cells showed robust contrast enhancement than control cells in the hollow fiber (Figure 6C).

We implanted β-cells in the encapsulated devices subcutaneously into a nude mouse. For comparison, two fiber membranes, one containing control cells and the other with labeled cells, were implanted at the opposite side of the mouse spine. Shortly after the implantation, we examined this mouse by T-1 weighed MR imaging. Labeled β-cells appeared to be very bright and could be clearly distinguished from the host mouse (Figure 7A-C). In contrast, control cells appeared to be much dimmer and the image intensity of these cells was about the same as the surrounding tissues of the host mouse. To address the question of how long these lipophilic Gd^{3+} agents remain on labeled cells in vivo, we repeated MR imaging of the mouse on days 3, 8, and 15 after implantation. In all experiments, labeled β-cells showed higher image intensity than the control unlabeled cells (Figure 7D−L), suggesting that Gd/DTPA−PDA−C_{12} could be used to label and to track cells in vivo for at least a few weeks.

3. Discussion

Prior to this report, the only method available for labeling cells with Gd^{3+} chelates for MR imaging applications involves using cell translocation peptides to shuttle covalently linked Gd^{3+} complexes across cell membranes.[16,17] By comparison, a variety of techniques have been developed to label cells with *T*2 agents based on superparamagnetic iron oxide (SPIO). These include exploiting fluid phase endocytosis or receptor mediated endocytosis,[11,43,44] using transfection reagents such as FuGENE or Lipofectamine,[12,13] nonspecific adhering of magnetodendrimers to cell membranes,[15] and employing HIV Tat peptides,[14] etc. The lack of efficient methods for labeling cells with T1 contrast agents such as Gd^{3+} chelates is due, at least in part, to the fact that relatively high concentrations of Gd^{3+}, typically on the order of millimolar or hundreds of micromolar, are required to achieve a robust contrast enhancement. Since there are many iron crystals in each SPIO nanoparticle,[9] the number of SPIO particles that need to be delivered into cells to produce a reliable contrast enhancement should be much less than the number of Gd^{3+} chelates.

We devised an alternative strategy of tagging cells with Gd^{3+} chelates by targeting cell membranes with lipophilic contrast agents. The success of this development relies on creating a

(36) Moore, A.; Bonner-Weir, S.; Weissleder, R. *Diabetes* **2001**, *50*, 2231−2236.
(37) Grimm, J.; Potthast, A.; Wunder, A.; Moore, A. *Int. J. Cancer* **2003**, *106*, 806−811.
(38) Moore, A.; Sun, P. Z.; Cory, D.; Hogemann, D.; Weissleder, R.; Lipes, M. A. *Magn. Reson. Med.* **2002**, *47*, 751−758.
(39) Jirak, D.; Kriz, J.; Herynek, V.; Andersson, B.; Girman, P.; Burian, M.; Saudek, F.; Hajek, M. *Magn. Reson. Med.* **2004**, *52*, 1228−1233.
(40) Fowler, M.; Virostko, J.; Chen, Z.; Poffenberger, G.; Radhika, A.; Brissova, M.; Shiota, M.; Nicholson, W. E.; Shi, Y.; Hirshberg, B.; Harlan, D. M.; Jansen, E. D.; Powers, A. C. *Transplantation* **2005**, *79*, 768−776.
(41) Lanza, R. P.; Chick, W. L. *Ann. N. Y. Acad. Sci.* **1997**, 831, 323−331.
(42) Newgard, C. B.; Clark, S.; BeltrandelRio, H.; Hohmeier, H. E.; Quaade, C.; Normington, K. *Diabetologia* **1997**, *40*, S42−47.
(43) Moore, A.; Weissleder, R.; Bogdanov, A. *J. Magn. Reson. Imaging* **1997**, *7*, 1140−1145.
(44) Bulte, J. W.; Zhang, S.; van Gelderen, P.; Herynek, V.; Jordan, E. K.; Duncan, I. D.; Frank, J. A. *Proc. Natl. Acad. Sci. U.S.A.* **1999**, *96*, 15256−15261.

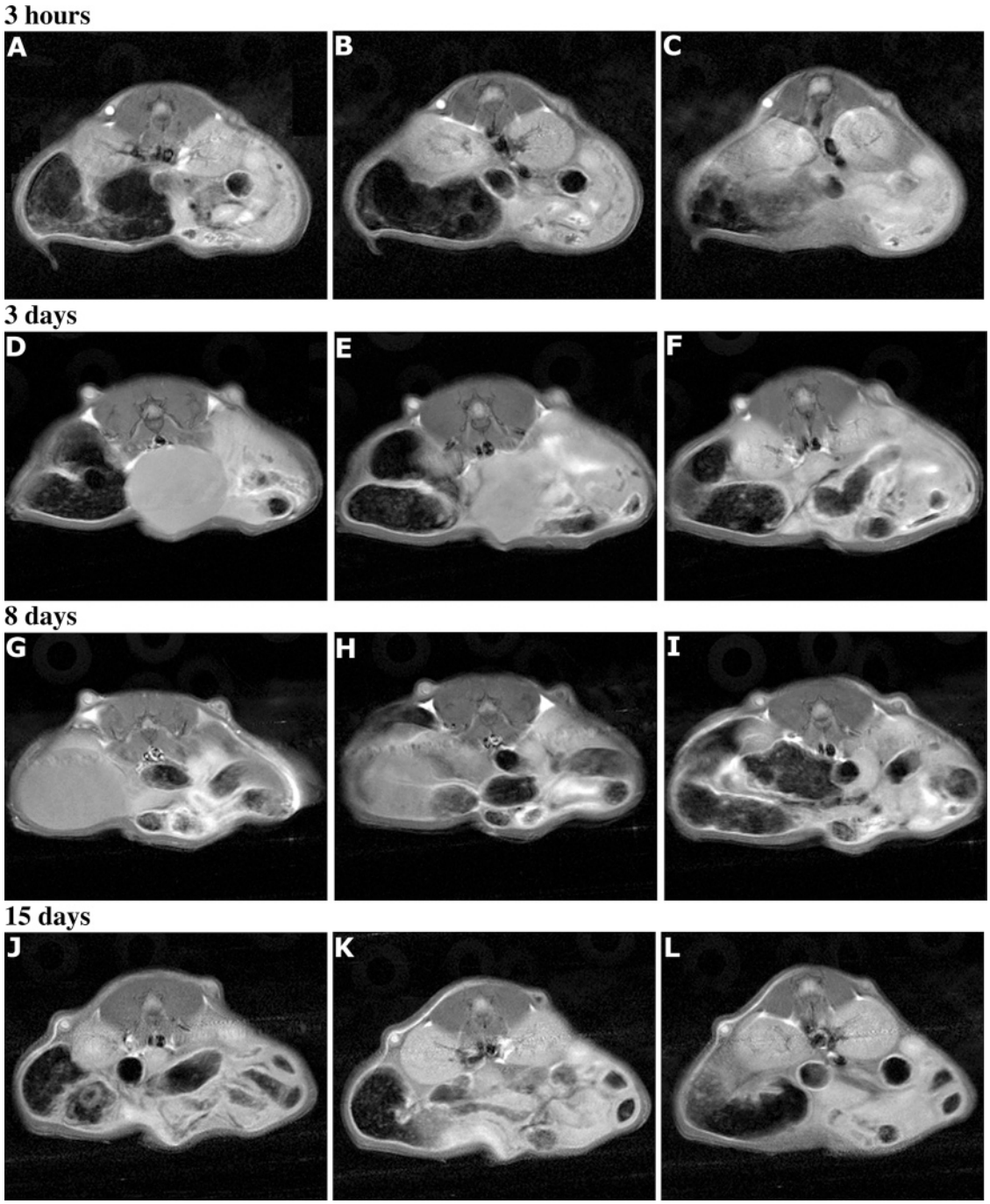

Figure 7. Tracking implanted INS-1 β-cells by MRI. (A−C) Contiguous transaxial images of a nude mouse 3 h after implantation. Labeled (left) and unlabeled β-cells (right) in encapsulated hollow fibers were transplanted subcutaneously. The same mouse was imaged again 3 days (D−F), 8 days (G−I), and 15 days (J−L) later. TR/TE = 900/25 ms.

new class of macrocyclic lanthanide ligands, DTPA−PDA−C_n. The molecular architecture of these ligands allows us to modify their structures and thus their hydrophobicities in a systematic manner. Gd^{3+} contrast agents prepared from these ligands label cells very efficiently: incubating cells with Gd/DTPA−PDA-C_n (n = 10 or 12) at micromolar concentration for less than an hour is sufficient to generate a visible intensity increase in $T1$-weighed MR images. This high labeling efficiency is in striking contrast with a recent report in which cells were labeled with a small hydrophilic contrast agent, Gd−HPDO3A (Prohance).[45] In that study, cells were incubated with Gd−HPDO3A at concentration higher than10 mM for more than 16 h at 37 °C. Presumably cells gradually accumulate Gd−HPDO3A through the process of pinocytosis.[45]

The membrane localization of these lipophilic complexes was confirmed by measuring DEFRET between Tb/DTPA−PDA−C_{10} and calcein. To our knowledge, this is the first report of applying the technique of DEFRET to study the localization of lanthanide complexes in living cells. This method is easy to perform and is very sensitive. Because of the long luminescence lifetime of lanthanide complexes, measuring DEFRET in the time-resolved mode is not susceptible to interference from short-

(45) Crich, S. G.; Biancone, L.; Cantaluppi, V.; Duo, D.; Esposito, G.; Russo, S.; Camussi, G.; Aime, S. *Magn. Reson. Med.* **2004**, *51*, 938−944.

lived background fluorescence or from the direct excitation of acceptor fluorophores. The sharply spiked emission of lanthanide ions facilitates distinguishing their signals from the emission of acceptors. In addition, the dipole moment of excited Tb^{3+} is randomized so the uncertainty caused by the angular dependence of energy transfer on the transition dipole moments is minimum. These combined advantages make DEFRET a sensitive and robust technique for detecting intermolecular interactions.

The efficacy of cell labeling and contrast enhancement of this class of lipophilic contrast agents appears to be general. A number of cultured mammalian cells, including both adhering and nonadhering cells, take up Gd/DTPA−PDA−C_{12} and Gd/DTPA−PDA−C_{10} efficiently. Labeled cells showed robust contrast enhancement over control cells. In addition, we were able to follow INS-1 cells labeled with Gd/DTPA−PDA−C_{12} by MRI for up to two weeks after implantation, suggesting that the Gd^{3+} complex remained to be associated with labeled cells in vivo. Such a stable labeling is required for the repetitive imaging of cells over a period of time. More hydrophobic homologues containing longer alkyl chains (Gd/DTPA−PDA−C_n, $n > 12$) may label cells and enhance image contrast for even longer durations. DiI, a lipophilic fluorescent label, contains two octadecyl alkyl chains ($C_{18}H_{37}$). When DiI was used as a retrograde tracer in adult nervous system, neurons remained labeled with DiI for up to 9 months without apparent leakage of the tracer to other neuronal cells.[20] The remarkably stable labeling most likely results from favorable hydrophobic interactions between alkyl chains and membrane lipids. Once taken up by cells, the enthalpy cost of moving two long alkyl chains out of membranes may be too high for DiI to escape from labeled cells. Over time these lipophilic dyes may be transported inside cells through the process of endocytosis.[18] This may further lengthen the duration of cell labeling. The gradual decline in the signal intensity of labeled cells may be caused by the slow release of Gd^{3+} ion from the chelates. The leakage of Gd^{3+} ion from chelates has been shown to occur in several clinically approved MRI contrast agents.[46−48] A possible solution to the problem is to label cells with both Gd/DTPA−PDA−C_n and excess chelates DTPA−PDA−C_n. The excess chelates may take up Gd^{3+} ions escaped from neighboring complexes to slow the leakage process and prolong the labeling time. We estimate that the stability constants of these macrocyclic Gd^{3+} complexes are on the order of 10^{16} to 10^{20} based on several reported Gd^{3+} complexes employing DTPA-bisamide as ligands.[46,49,50] These DTPA-bisamide chelates also bind to Gd^{3+} with good selectivity against competing physiological cations such as Ca^{2+} and Zn^{2+}. Studies by Raymond and co-workers suggested that amide functional groups of DTPA-bisamide ligands contribute to the stability of Gd^{3+} complexes.[51] Future studies will quantify the metal stability constants of these macrocyclic complexes.

In addition to labeling cultured cells in vitro, Gd/DTPA−PDA−C_n can also be applied to label primary cells in tissues. We have shown that pancreatic islets could be labeled with Gd/DTPA−PDA−C_{12} in about an hour. The fast labeling kinetics is a major advantage of this new class of cyclic contrast agents. To label cells with magnetic dyes in situ in living organisms, it is important to have cells take up topically applied magnetic labels in a relatively short period of time. This type of studies is of particular interest to developmental biologists. DiI and DiO have been used to label migrating neuronal cells in developing embryos of several model organisms.[52,53] Gd/DTPA−PDA−C_n can probably be applied in a similar manner to follow the migration trajectory of labeled cells at depths beyond the detection limit of optical microscopy. In addition, to selectively label a sub-population of cells in vivo, one would like to obtain relaxation regents with higher cellular targeting specificity. A promising approach in this area involves using engineered antibodies that irreversibly bind to electrophilic ligands to achieve covalent labeling.[54] Finally, new proto-type of contrast agents with higher molecular relaxivity have recently been reported.[55] Since these Gd^{3+} complexes are predicted to be more effective in enhancing image contrast than agents derived from DTPA or DOTA ligands, they may also serve as useful templates to develop new cellular labels. Lower doses of contrast agents with high relaxivity would be needed for imaging applications, thus providing a solution to reduce the potential long-term toxicity of metal complexes.

In summary, we have developed a novel class of macrocyclic lanthanide chelates suitable for cell labeling and imaging applications. Ln/DTPA−PDA−C_n can be conveniently prepared from easily accessible starting materials. The simplicity of the labeling procedure, the efficiency of cellular uptake, and the efficacy of contrast enhancement are unique and desirable features of this class of lipophilic contrast agents. The combination of these advantages provides a valuable technique for labeling cells with T1 contrast agents consisting Gd^{3+}. Future developments and optimization of these cellular labeling and targeting strategies should provide more specific and less invasive means for MR imaging applications. Combining with 3-dimensional MRI microscopy, these agents are expected to have broad applications in imaging cell movement and localization in different biological systems in vivo.

4. Experimental Section

4.1. Organic Syntheses. All reagents were purchased from Aldrich or Fluka. Anhydrous solvents were stored over activated molecular sieves (3 or 4 Å). Thin-layer chromatography (TLC) was performed on precoated silica gel 60F-254 glass plates (EM Science). Reaction products were purified by low-pressure flash chromatography (FC) using silica gel 60 (63∼200 μm, EM Science), or reverse phase chromatography (Lichroprep RP-18, EM Separations), or ion exchange chromatography (Chelex 100, BioRad). ^{1}H NMR spectra were acquired on Varian 300 or 400 MHz spectrometers. Chemical shifts (δ, ppm) were reported against tetramethylsilane (0 ppm). MALDI-TOF Mass Spectroscopy was performed on a Voyager-DE PRO biospectrometry workstation (Applied Biosystems) using 2,5-dihydroxy benzoic acid as the matrix. High-Pressure Liquid Chromatography (HPLC) analysis was performed on a Shimadzu HPLC system (SCL-10A vp controller) equipped with an auto-injector, a photodiode array detector, and a

(46) Cacheris, W. P.; Quay, S. C.; Rocklage, S. M. *Magn. Reson. Imaging* **1990**, *8*, 467−481.
(47) Tweedle, M. F.; Hagan, J. J.; Kumar, K.; Mantha, S.; Chang, C. A. *Magn. Reson. Imaging* **1991**, *9*, 409−415.
(48) Kirchin, M. A.; Runge, V. M. *Top. Magn. Reson. Imaging* **2003**, *14*, 426−435.
(49) Carvalho, J. F.; Kim, S. H.; Chang, C. A. *Inorg. Chem.* **1992**, *31*, 4065−4068.
(50) Imura, H.; Choppin, G. R.; Cacheris, W. P.; deLearie, L. A.; Dunn, T. J.; White, D. H. *Inorg. Chim. Acta* **1997**, *258*, 227−236.
(51) Paulroth, C.; Raymond, K. N. *Inorg. Chem.* **1995**, *34*, 1408−1412.
(52) Bossing, T.; Technau, G. M. *Development* **1994**, *120*, 1895−906.
(53) Kulesa, P. M.; Fraser, S. E. *Dev. Biol.* **1998**, *204*, 3273−44.
(54) Corneillie, T. M.; Lee, K. C.; Whetstone, P. A.; Wong, J. P.; Meares, C. F. *Bioconjug. Chem.* **2004**, *15*, 1392−1402.
(55) Raymond, K. N.; Pierre, V. C. *Bioconjug. Chem.* **2005**, *16*, 3−8.

fluorescence detector. An analytical reverse phase column (250 × 4.6 mm, Luna C-18/5 μm, Phenomenex, Torrance, CA) was used.

2,6-Bis[(*N*,*N*′-di(trifluoroacetyl)-*N*,*N*′-dibutyl)-aminomethyl]pyridine (2a). 2,6-Bis(bromomethyl) pyridine (265 mg, 1 mmol) dissolved in dry toluene (2 mL) was mixed with excess butylamine (5.1 mL, 52.0 mmol) under Argon. After stirring at room temperature (r.t.) for 6 h, the solvent was removed to give a colorless oil. The excess butylamine was removed under high vacuum to give diamine **1a**. This was used directly for the next step without further purification.

The crude mixture containing **1a** was mixed with potassium carbonate (552 mg, 4 mmol) and trifluoroacetic anhydride (0.85 mL, 6 mmol) in anhydrous acetonitrile (5 mL). After stirring at r.t. for 4 h under argon, the solvent was removed under vacuum. The residue was extracted with ethyl acetate/H_2O. The organic layer was dried over anhydrous Na_2SO_4. After evaporating the solvent, the oily residue was purified by FC (Hexane/Ethyl Acetate, 2:1). The product was obtained as a brown oil (310 mg, 70%). ^{1}H NMR (300 MHz, δ ppm, $CDCl_3$): 7.76−7.92(m, 1H), 7.14−7.37(m, 2H), 4.73−4.83(m, 4H), 3.36−3.51-(m, 4H) 1.50−1.68(m, 4H), 1.23−1.36(m, 4H), 0.92(t, J = 7.2 Hz, 6H).

2,6-Bis[(*N*,*N*′-di(trifluoroacetyl)-*N*,*N*′-didecyl)-aminomethyl]pyridine (2b). 2,6-Bis(bromomethyl) pyridine (200 mg, 0.76 mmol) dissolved in dry toluene (3 mL) was added to an excess of decylamine (0.9 mL, 4.53 mmol). After stirring at r.t. overnight, the solvent was removed under high vacuum to give an oil. The crude mixture was dissolved in anhydrous acetonitrile (6 mL). Potassium carbonate (834 mg, 6 mmol) and trifluoroacetic anhydride (1.06 mL, 7.55 mmol) were then added under argon. After stirring at r.t. overnight, the solvent was removed under vacuum. The residue was first purified by FC (Hexane/Ethyl Acetate, 5:1) to remove salts. Fractions containing the product were pooled, concentrated and carefully purified again by FC (Hexane/Ethyl Acetate, 30:1). The product was obtained as a pale yellow oil (265 mg, 58%). ^{1}H NMR (300 MHz, δ ppm, $CDCl_3$): 7.62−7.80(m, 1H), 7.07−7.20(m, 2H), 4.67−4.70(m, 4H), 3.34−3.52(m, 4H), 1.50−1.63(m, 4H), 1.2−1.4(m, 28H), 0.87(t, J = 6.0 Hz, 6H).

2,6-Bis[(N,N′-di(trifluoroacetyl)-N,N′-didodecyl)-aminomethyl]-pyridine (2c). Compound **2c** was synthesized similarly from dodecylamine in 50% yield. ^{1}H NMR (300 MHz, δ ppm, $CDCl_3$): 7.62−7.75-(m, 1H), 7.07−7.21(m, 2H), 4.67−4.70(m, 4H), 3.35−3.49(m, 4H), 1.55−1.63(m, 4H), 1.2−1.39(m, 36H), 0.87(t, J = 5.1 Hz, 6H).

DTPA−PDA−C_4. NaOH (27.4 μL, 10N, 0.274 mmol) was added to a solution of **2a** (60.4 mg, 0.137 mmol) in 1.5 mL THF. The mixture was stirred at 50 °C under argon for 6 h. The solvent was then removed under vacuum to yield a yellow solid. The solid containing diamine **1a** was suspended in dry DMF (10 mL). DTPA dianhydride (48.9 mg, 0.137 mmol) in 20 mL DMF was slowly added. The mixture was stirred at r.t. under argon for 24 h. After removing DMF under high vacuum, the residue was purified by reversed-phase-C_{18} chromatography eluting with MeOH/H_2O. The product was obtained as a glass after removing solvent (32 mg, 39%). ^{1}H NMR (400 MHz, δ ppm, D_2O): 7.82(t, J = 7.5 Hz, 1H), 7.36(m, 2H), 4.4(m, 4H), 3.84(m, 4H), 3.63(s, 2H), 3.2−3.5(m, 16H), 1.38−1.58(m, 4H), 1.16−1.32(m, 4H), 0.79−0.88(m, 6H). MS: 606.34 calcd. for $C_{29}H_{46}N_6O_8$; obsd.: 607.04 $[M+H]^+$, 629.01 $[M+Na]^+$, 645.00 $[M+K]^+$.

DTPA−PDA−C_{12} and DTPA-PDA-C_{10} were synthesized similarly from **2b** and **2c**, respectively, in about 25% yields.

DTPA−PDA−C_{10}. ^{1}H NMR (400 MHz, δ ppm, CD_3OD): 7.67−7.71(m, 1H), 7.17−7.22(m, 2H), 4.55−4.62(m, 4H), 4.10−4.22(m, 4H), 3.94−4.02(m, 4H), 3.53(s, 2H), 3.10−3.32 (m, 12H), 1.36−1.44(m, 4H), 1.18−1.3(m, 28H), 0.86(t, J = 5.1 Hz, 6H). MS: 774.53 calcd. for $C_{41}H_{70}N_6O_8$; obsd.: 775.33 $[M+H]^+$, 797.34 $[M+Na]^+$, 813.32 $[M+K]^+$.

DTPA−PDA−C_{12}. ^{1}H NMR (400 MHz, δ ppm, CD_3OD): 7.63−7.80(m, 1H), 7.18−7.28(m, 2H), 4.58−4.64(m, 4H), 2.85−3.88(m, 22H), 1.42−1.58(m, 4H), 1.2−1.4(m, 36H), 0.89(t, J = 5.1 Hz, 6H). MS: 830.59 calcd. for $C_{45}H_{78}N_6O_8$; obsd.: 831.56 $[M+H]^+$, 853.55 $[M+Na]^+$.

Preparing Ln^{3+} Complexes of DTPA−PDA−C_n. An aqueous solution of $LnCl_3$ (1.2 equivalent) was mixed with DTPA−PDA−C_n in MeOH. The mixture was stirred at r.t. for 8 h during which aliquots of 0.1 N NaOH were added to maintain the pH around 6.5. Excess Ln^{3+} ions were removed by passing the reaction mixture through an ion exchange column (Chelex 100, BioRad). Fractions containing the product were pooled, concentrated, and purified again by reversed-phase-C_{18} chromatography eluting with MeOH/H_2O (30% to 90% MeOH). Because lanthanide chelates are overall neutral, they have longer retention times on the reverse phase C_{18}-column than the corresponding free ligands, and they could be isolated to high purity using this method. An example of HPLC analysis of DTPA−PDA−C_{10} and Tb/DTPA−PDA−C_{10} is shown in Figure S3 (Supporting Information).

Tb/DTPA−PDA−C_4. MS: 762.24 calcd. for $C_{29}H_{43}N_6O_8Tb$; obsd.: 763.10 $[M+H]^+$, 785.08 $[M+Na]^+$, 801.07 $[M+K]^+$.

Tb/DTPA−PDA−C_{10}. MS: 930.43 calcd. for $C_{41}H_{67}N_6O_8Tb$; obsd.: 931.48 $[M+H]^+$, 953.47 $[M+Na]^+$, 969.48 $[M+K]^+$.

Tb/DTPA−PDA−C_{12}. MS: 986.49 calcd. for $C_{45}H_{75}N_6O_8Tb$; obsd.: 987.66 $[M+H]^+$, 1009.63 $[M+Na]^+$.

Gd/DTPA−PDA−C_4. MS: 761.24 calcd. for $C_{29}H_{43}N_6O_8Gd$; obsd.: 761.99 $[M+H]^+$ (major isotopic peaks include 758.00, 759.01, 760.98,761.99, 763.00, 764.00 and 765.00), 783.99 $[M+Na]^+$.

Gd/DTPA−PDA−C_{10}. 929.43 calcd. for $C_{41}H_{67}N_6O_8Gd$; obsd.: 930.35 $[M+H]^+$ (major isotopic peaks include 927.66, 928.35, 929.36, 930.35, 931.37 and 932.35), 952.33 $[M+Na]^+$.

Gd/DTPA−PDA−C_{12}. 985.49 calcd. for $C_{45}H_{75}N_6O_8Gd$; obsd.: 986.51 $[M+H]^+$ (major isotopic peaks include 983.53, 984.50, 985.52, 986.81, 987.51, 988.52, 989.52 and 990.53), 1008.52 $[M+Na]^+$.

4.2. Cell Culturing and Labeling. Cells were grown at 37 °C and 5% CO_2 in a humidified atmosphere. Hela cells were cultured in high glucose (25 mM) DMEM medium (Gibco) containing 10% fetal bovine serum (FBS). INS-1 cells (832/13 clone[56]) was a generous gift from Dr. Christopher Newgard. These cells were cultured in RPMI 1640 medium (Gibco) supplemented with 10% FBS, 11 mM glucose, 10 mM Hepes, 2 mM L-glutamine, 1 mM sodium pyruvate, and 50 μM β-mercaptoethanol. Jurkat cells (clone E6−1, American Type Culture Collection, Manassas, VA) were cultured in RPMI 1640 medium supplemented with 10% FBS, 25 mM glucose, 10 mM Hepes, 2 mM L-glutamine, and 1 mM sodium pyruvate. All culture mediums contain 100 U/mL penicillin and 100 μg/mL streptomycin. Cells were passed every 3−5 days.

Cells grown to nearly 100% confluence were labeled with lanthanide complexes. Cells were first washed twice with Hanks Balanced Saline (HBS, Gibco) containing 10 mM Hepes (pH 7.30) and 5.5 mM glucose. Jurkat cells were collected by centrifugation after each washing (300 rpm for 3 min on a benchtop centrifuge). Stock solutions of Ln/DTPA-PDA-C_n prepared in DMSO or EtOH were first mixed with a small volume of HBS. The mixture was then added to cells bathed in HBS. The amount of DMSO or EtOH is kept below 0.2%. We usually loaded cells for 40−60 min before washing them several times with HBS.

4.3. Spectroscopic Characterization of Tb^{3+} Complexes and Measuring DEFRET. UV−vis spectra were recorded in a 1 cm path quartz cell on a Shimadzu 2401 PC spectrometer. Steady state and time-resolved fluorescence spectra were recorded on a LS-55B Luminescence Spectrometer (Perkin-Elmer). In the time-resolved mode, a delay time (t_d) of 0.1 ms and a gate time (t_g) of 1 ms were used. To study the cellular localization of Tb/DTPA−PDA−C_{10} by DEFRET, we labeled about 2 million Jurkat cells in 1 mL HBS with Tb/DTPA−PDA−C_{10} (10 μM) at r.t. for 40 min. Labeled cells were washed twice with HBS

(56) Hohmeier, H. E.; Mulder, H.; Chen, G.; Henkel-Rieger, R.; Prentki, M.; Newgard, C. B. *Diabetes* **2000**, *49*, 424−430.

and resuspended in HBS. The time-resolved spectrum of labeled cells was recorded. Calcein was then added to the cell suspension in 1 μM increment. After each addition, gated emission spectra were recorded. Alternatively, Jurkat cells were coloaded with calcein/AM (1 μM) and Tb/DTPA−PDA−C_{10} (10 μM). Intracellular delivery of calcein from calcein/AM was confirmed by fluorescence imaging (Carl Zeiss Axiovert 200 microscope) of labeled cells on a glass cover slip coated with polylysine (0.1%).

4.4. MR Imaging of Labeled Cells in Vitro and in Nude Mice after Implantation. MR imaging experiments were carried out on a Varian Unity INOVA wide bore (~40 cm) imaging system equipped with an Oxford 4.7 T magnet. The images were acquired using a standard spin−echo sequence with T1-weighing. Hela, INS-1 832/13 and other adhering cells labeled with Gd/DTPA−PDA−C_n were detached from culture dishes using Trypsin-EDTA (0.05%). The cell suspension was then transferred to a small vial. After centrifugation and removal of Trypsin-EDTA solution, HBS was slowly added to cover the cell pellet (20−100 millions of cells). Vials containing cell pellets were placed vertically next to each other on a foam stand and imaged together.

Human islets were obtained through the Human Islet Distribution Program supported by the Juvenile Diabetes Research Foundation (JDRF). Islets were cultured in CMRL medium (Mediatech, Inc) supplemented with 10% FBS. They were kept at 22 °C with 5% CO_2 at low density (1000 islet equivalents/mL). Prior to labeling, about 10 000 islet equivalents were first washed with serum free medium. They were then incubated with Gd/DTPA−PDA−C_{12} (20 μM) in 1.5 mL of CMRL medium for 60 min with gentle shaking. After loading, islets were washed several times with CMRL medium and collected by centrifugation in 0.6 mL vials. The islet pallets at the bottom of vials were covered with CMRL medium prior to MR imaging.

To implant and image beta-cells in nude mice, INS-1 832/13 cells were labeled with Gd/DTPA−PDA−C_{12}. Labeled cells were washed with HBS, detached with Trypsin−EDTA, and resuspended in a roughly equal volume of HBS. The cell suspension was injected into the Cellmax Implant Membrane Hollow Fiber (Spectrumlabs, Rancho Dominguez, CA). The hollow fiber was about 25 mm in length, and it was heat sealed at both ends after cells were injected. The Cellmax Implant Membranes are made from modified poly(vinylidene difluoride) (PVDF) and have pores with a molecular weight cutoff of 500 KD. We implanted two pieces of fibers, one containing control unlabeled cells and the other with labeled cells, by inserting fibers through craniodorsal skin incisions (3 mm) into the subcutaneous tissues of an adult nude mouse. The skin incisions were then closed with a bandage. The implanted fibers were placed in parallel to the spine. The mouse was subjected to MR imaging 3 h after the implantation and then on days 3, 8, and 15. During implantation and imaging, the mouse was anesthetized with 1.5% isoflurane (Baxter Caribe Inc., Deerfield, IL) through a nose cone perfusing oxygen at a rate of 0.2 L/min (Ohmeda VMC Anesthesia Machine). Transaxial contiguous slices of 3 mm thickness were obtained over the mouse body covering the implanted fibers. The field of view was 45 mm, and the matrix size was 256 × 256 pixels.

Acknowledgment. This research was supported by research grants from the Welch Foundation (I-1510) and from the National Institute of Health (DK063525) to W-h. Li. We thank Dr. Christopher Newgard (Duke University) for providing 832/13 INS-1 cells. We also thank Drs. Kathlynn Brown and Thomas Kodadek for providing us the access to the MALDI-TOF mass spectrometer.

Supporting Information Available: MR images of labeled cells, absorption spectrum of a ligand, and HPLC analysis of purified chelates. This material is available free of charge via the Internet at http://pubs.acs.org.

JA054593V